ISSN 0208-7774 TRIBOLOGIA 3/2023 p. 43–51
DOI: 10.5604/01.3001.0053.9435

Katarzyna PIOTROWSKA[*], Monika MADEJ[**]

TRIBOLOGICAL PROPERTIES OF SILVER DOPED TITANIUM NITRIDE COATINGS

WŁAŚCIWOŚCI TRIBOLOGICZNE POWŁOK AZOTKU TYTANU DOMIESZKOWANYCH SREBREM

Key words: PVD technique, titanium alloys, surface texture, friction, wear, adhesion.

Abstract: The properties of titanium nitride (TiN:Ag) coatings applied by physical vapour phase deposition technique (PVD) on Ti13Nb13Zr alloy were subject to evaluation. The study presents the results of surface geometrical structure, adhesion and tribological tests. The geometric structure of the surface was examined using optical microscopy. A scratch test was used to assess adhesion. The model tribological tests were carried out in a rotary motion under technically dry friction conditions, lubricated with Ringer's solution. In the case of technically dry friction, the analysis of the tribological test results indicated that the TiN:Ag coating was characterised by higher resistance to motion and lower wear compared to Ti13Nb13Zr. Friction coefficients registered during friction subject to lubrication with Ringer's solution were compared for both materials; however, the surface wear was significantly lower in titanium alloy. The scratch test pointed towards high adhesion of the TiN:Ag coating. The study results provide insight into Ti13Nb13Zr alloy, titanium nitride coatings and their potential use for surgical instruments.

Słowa kluczowe: PVD, stopy tytanu, struktura geometryczna powierzchni, tarcie, zużycie, adhezja.

Streszczenie: Ocenie poddano właściwości powłok azotku tytanu (TiN:Ag) naniesionych metodą fizycznego osadzania z fazy gazowej PVD na stopie Ti13Nb13Zr. Przedstawiono wyniki badań struktury geometrycznej powierzchni, adhezji oraz testów tribologicznych. Strukturę geometryczną powierzchni zbadano przy użyciu mikroskopii optycznej. Do oceny adhezji wykorzystano test zarysowania, tzw. scratch test. Modelowe badania tribologiczne przeprowadzono w ruchu obrotowym w warunkach tarcia technicznie suchego oraz ze smarowaniem płynem Ringera. Analiza wyników badań tribologicznych wskazała, że w przypadku tarcia technicznie suchego powłoka charakteryzowała się jedocześnie większymi oporami ruchu i mniejszym zużyciem w porównaniu z Ti13Nb13Zr. Współczynniki tarcia zarejestrowane podczas tarcia ze smarowaniem roztworem Ringera były porównywane dla obu materiałów, z kolei zużycie powłoki było dużo mniejsze w odniesieniu do stopu tytanu. Test zarysowania wskazał na wysoką adhezję powłoki TiN:Ag. Uzyskane wyniki badań stanowią źródło wiedzy na temat stopu Ti13Nb13Zr, powłok azotku tytanu oraz możliwości ich potencjalnego zastosowania na narzędzia chirurgiczne.

INTRODUCTION

Medicine is one of the most rapidly developing scientific domains. Technological advances in the form of improved diagnostic techniques have led to the introduction of advanced surgical equipment. Surgery, where modern solutions in materials and design are readily used, is an integral part of most medical specialities. This is mainly the case for surgical instruments, a group of specialised instruments used in both soft tissue and hard tissue surgery. Given the type of work performed, they can be categorised under the following groups: cutting tools, gripping tools, displacement tools,

[*] ORCID: 0000-0001-6366-2755. Kielce University of Technology, Faculty of Mechatronics and Mechanical Engineering, Tysiąclecia Państwa Polskiego 7 Ave., 25-314 Kielce, Poland.
[**] ORCID: 0000-0001-9892-9181. Kielce University of Technology, Faculty of Mechatronics and Mechanical Engineering, Tysiąclecia Państwa Polskiego 7 Ave., 25-314 Kielce, Poland.

pulling tools, and other tools (striking, penetrating, gripping) **[L. 1–3]**. Choosing the right tool will ensure the optimum working time and surgical wound size. It should be noted that the increased complexity of the surgical procedure causes an increase in the price of the tools.

Geometry, ergonomics, sterilisation resistance and resistance to body fluids are all requirements for surgical instruments. The ergonomics are essential for the safety of the operator and the patient, as well as the reliability and failure-free operation **[L. 2]**. The conditions specified above determine the choice of material, which should ensure their reliable operation **[L. 4–5]**. Initially, martensitic and austenitic steels were used to manufacture surgical instruments. Modern engineering materials such as titanium and its alloys have replaced them over time **[L. 6–7]**. Good mechanical properties, a high level of corrosion resistance in comparison with other materials, and biocompatibility characterise these metals. Surgical instruments can be damaged or subject to excessive wear and tear from contact with tissue and body fluids, drugs, sterilising agents and disinfectants **[L. 3, 8–9]**. **Figure 1** shows the status of the medical instruments used in Poland's medical centres.

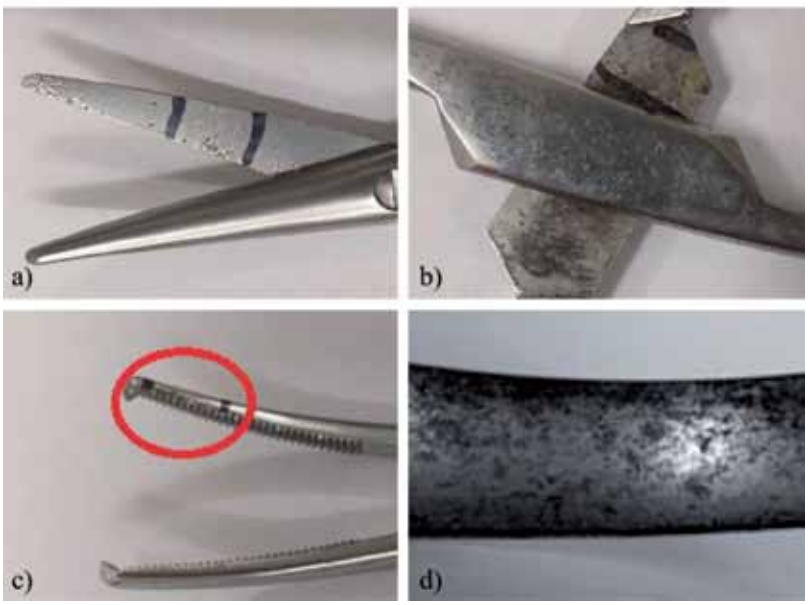

Fig. 1. Macroscopic images of surgical instruments (a) scissors, (b) clamp joint, (c) forceps, (d) hook [L. 11]
Rys. 1. Obrazy makroskopowe narzędzi chirurgicznych a) nożyczki, b) złącze imadła, c) kleszczyki, d) hak [L. 11]

Defects that preclude further use were identified during macroscopic observations of selected surgical instruments. Numerous chippings, scratches and pores are indicative of tribocorrosion wear were present in all cases examined. They resulted from an incorrect choice of material for the tool – the material did not show sufficient resistance to wear and corrosion. Casting defects may have been an additional factor that exacerbated the issue. **Figure 1c** shows a photograph of Kocher's forceps. Local plastic deformation of the material was observed on the tool surface, taking the form of a so-called burr. The observed change was not the result of technical defects in the material but rather caused by the improper use of the tool or an incorrect choice of material for the tool.

The image of the condition of surgical instruments in use in medical centres inspired the theme of surface modification of medical instruments. This article proposes applying a titanium nitride coating TiN:Ag with antiwear and antimicrobial properties on a Ti13Nb13Zr titanium alloy with high biocompatibility but insufficient tribological wear resistance.

MATERIALS AND METHODS

The TiN:Ag coating was applied on Ti13Nb13Zr titanium alloy using the PVD technique. The chemical composition of the alloy and its basic mechanical properties: tensile strength (R_m), yield

Table 1. Chemical composition of Ti13Nb13Zr titanium alloy, % wag [L. 12]
Tabela 1. Skład chemiczny stopu tytanu Ti13Nb13Zr w % wag **L. 12]**

Element	% weight							
	C	H	O	N	Fe	Nb	Zr	Ti
Ti13Nb13Zr	≤ 0,08	≤ 0,015	≤ 0,016	≤ 0,05	≤ 0,25	12,5-14,0	12,5-14,0	based

Table 2. Mechanical properties of the Ti13Nb13Zr alloy [L. 6]
Tabela 2. Właściwości mechaniczne stopu Ti13Nb13Zr **[L. 6]**

Material	$R_{m,}$ MPa	$R_{e,}$ MPa	A, %	E, GPa
Ti13Nb13Zr	973 – 1037	836 – 908	10 – 16	79 – 84

strength (R_e), A – elongation, and E – Young's modulus, are presented in **Tables 1** and **2.**

Prior to the deposition of the coatings, the discs, which are 30 mm in diameter and 5 mm in height, were ground and polished using a grinding and polishing machine made by Pace Technologies. Polishing was done with a 1 µm diamond paste. The last step was to degrease the samples in an ultrasonic cleaner in an environment with ethanol as the solvent. The amplitude parameters of the geometrical surface structure of the surfaces thus prepared are shown in **Table 3**.

A silver-doped titanium nitride coating was commissioned from an external company – Oerlikon Balzers. The coating is the result of a physical vapour deposition (PVD) process. The process involved the deposition of the coating in the presence of plasma at reduced pressures ranging from 10 to 10^{-5} Pa, at temperatures ranging from 150 to 500°C. This technique allows the formation of very thin films (in the order of a few micrometres), in which the interface between the coating and the substrate is generally of an adhesive–diffusion nature. The components were rotated at uniform speeds around several axes to achieve a uniform coating thickness.

The geometric structure of the surface before **(Fig. 4)** and after **(Fig. 9)** tribological testing was measured using a confocal microscope with Leica DCM8 interferometric mode. The dimensions of the observed area were 1.2 x 1.6 mm. The evaluation was carried out based on axonometric (3D) images of the surveyed surfaces, surface profiles and amplitude parameters (S_p, S_v, S_a, S_q, S_{sk}, S_{ku}).

Morphology studies using the Phenom XL scanning electron microscope included microscopic observations of the metallographic specimens in cross-section. From these, the deposited layer's thickness and chemical composition were determined **(Fig. 5)**. The test was carried out using an acceleration voltage of 15 kV and a magnification of x10000.

Tribological tests were carried out using an Anton Paar TRB^3 tribometer. The tests were carried out in rotary motion under technically dry friction and friction lubricated with Ringer's solution – a substance that simulates body fluid. A 1000 ml lubricant was prepared with the following substances: 8.6 g NaCl, 0.3 g KCl, 0.243 g $CaCl_2$ and distilled water. The counter specimen at the friction nodes was a sphere made of Al_2O_3 with a diameter of 6 mm. Tribological tests used a load of 1 N, a friction path of 1,000 m and a linear velocity of 0.1 m/s. A diagram of the friction pair is shown in **Fig. 2**. The tests were carried out three times for each pair of slides with the applied parameters. The friction coefficient and linear wear values were determined during the study. Microscopic observations were made on the samples using a Leica DCM 8 after the tribological tests.

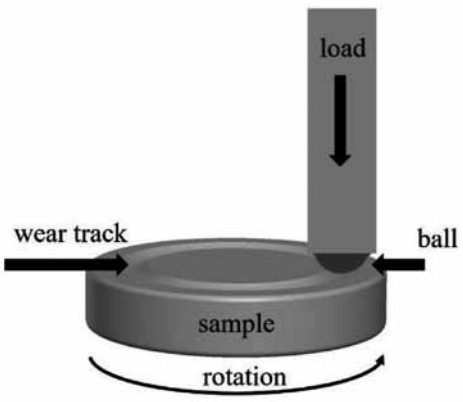

Fig. 2. Friction pair
Rys 2. Węzeł tarcia

The adhesion of the coating to the substrate is an essential criterion for the quality and durability of the deposited coating. The critical load LC – i.e., the force at which the coating breaks – can be determined from microscopic observation of the resulting scratch, recorded changes in the friction coefficient, normal force F_N or friction force F_T and the acoustic emission signal. The adhesion of the TiN:Ag coating to the substrate was measured using a scratch tester MCT^3 manufactured by Anton Paar. The layer was scratched with a Rockwell diamond indenter with a radius of curvature of 100 µm over a 3 mm section. A diagram of the scratch method is shown in **Figure 3**. Increasing load from 0.03 to 15 N was applied, and a constant table travel speed of 12 mm/min was used.

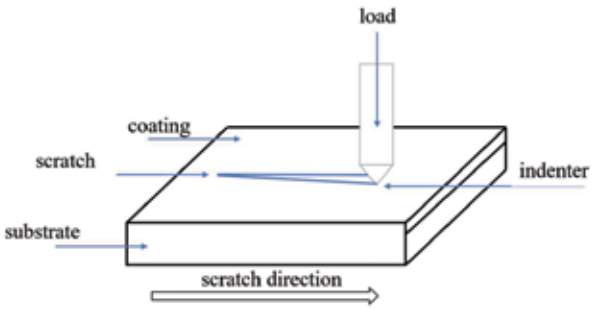

Fig. 3. Scratch diagram
Rys. 3. Schemat zarysowania

RESULTS

Axonometric (3D) images, mean surface profiles and amplitude parameters were used to assess the geometric structure of the surface.

Table 3. The parameters of surface texture
Tabela 3. Parametry amplitudowe

Parameter	Ti13Nb13Zr		TiN:Ag	
	mean	stand. dev.	mean	stand. dev.
S_p [nm]	192	0.17	3.89	0.28
S_v [nm]	0,99	0.11	2.61	0.42
S_a [nm]	0.08	0.001	0.1	0.001
S_q [nm]	0.1	0.003	0.11	0.005
S_{sk}	-0.14	0.05	1.03	0.07
S_{ku}	3.59	0.76	20.96	1.23

The analysis of the amplitude parameters showed that the titanium nitride coating has a more developed geometrical surface structure than the reference sample – a Ti13Nb13Zr alloy. The values of the parameters indicate this: *Sp* – maximum peak height and *Sv* – maximum depression depth. Both ratios are almost double that of the reference sample for the coating. The surface roughness of the cooperating parts directly influences the friction coefficient and the wear intensity. The tribological properties of the material can be predicted at the

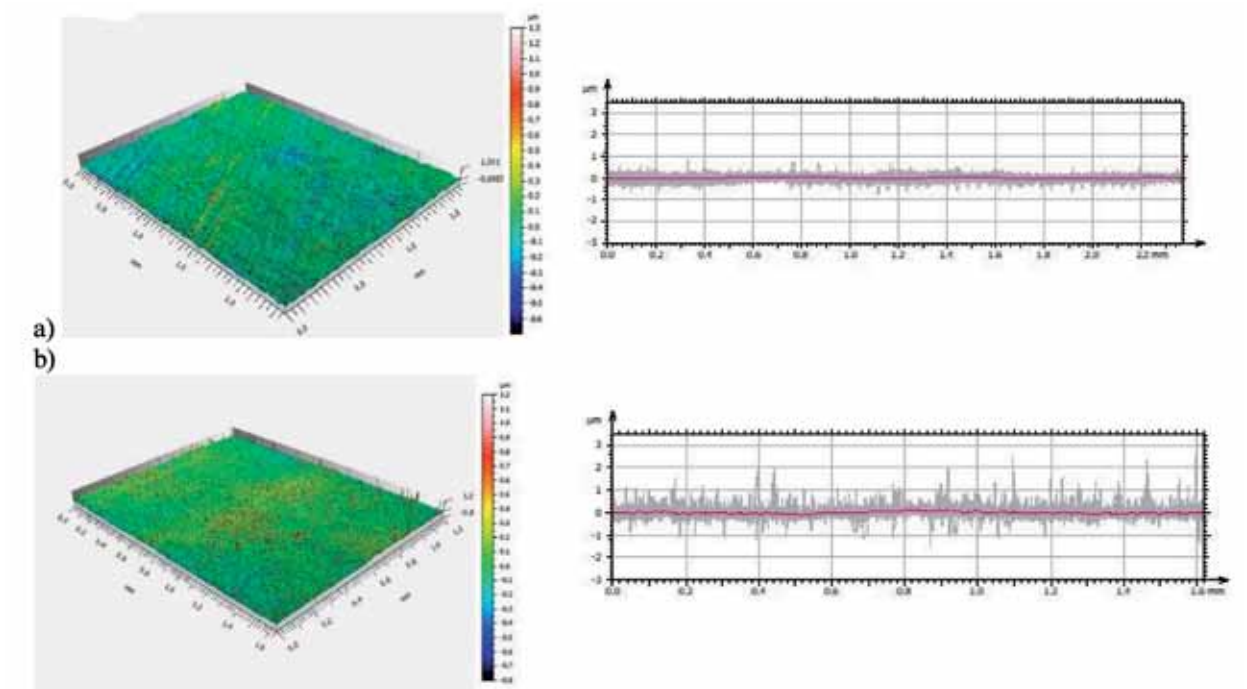

Fig. 4. The axonometric image of surface texture a) Ti13Nb13Zr, b) TiN:Ag
Rys. 4. Obrazy aksonometryczne i profile powierzchni struktury geometrycznej powierzchni a) Ti13Nb13Zr, b) TiN:Ag

surface layer deposition stage by detailed analysis of the geometrical structure of the surface.

A detailed quantitative and qualitative analysis of the deposited layer was performed using scanning electron microscopy. The thickness and nature of the deposited coating were assessed based on the metallographic sample, and the chemical composition was analysed. **Figure 5** shows an image of the microstructure of the coating with the thickness marked (**a**) and the results of the qualitative analysis of the chemical composition (**b**) and (**c**).

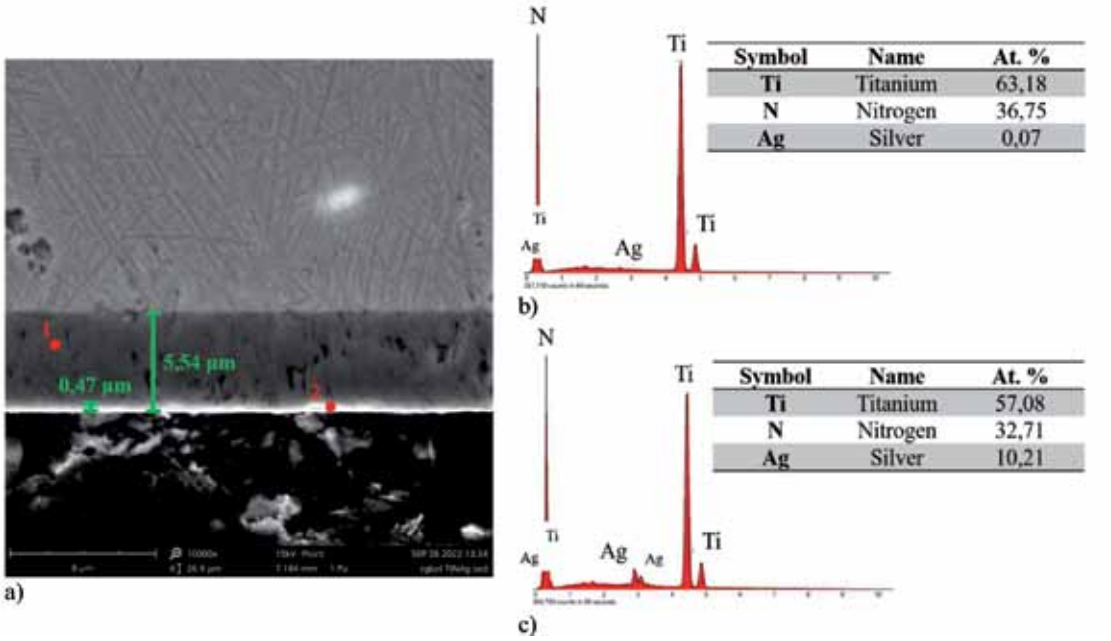

Fig. 5. Micrograph of TiN:Ag coating on cross-section (a), qualitative analysis results point 1 (b), qualitative analysis results point 2 (c)

Rys. 5. Mikrofotografia powłoki TiN:Ag na przekroju poprzecznym (a), wyniki analizy jakościowej w punkcie 1 (b), wyniki analizy jakościowej w punkcie 2 (c)

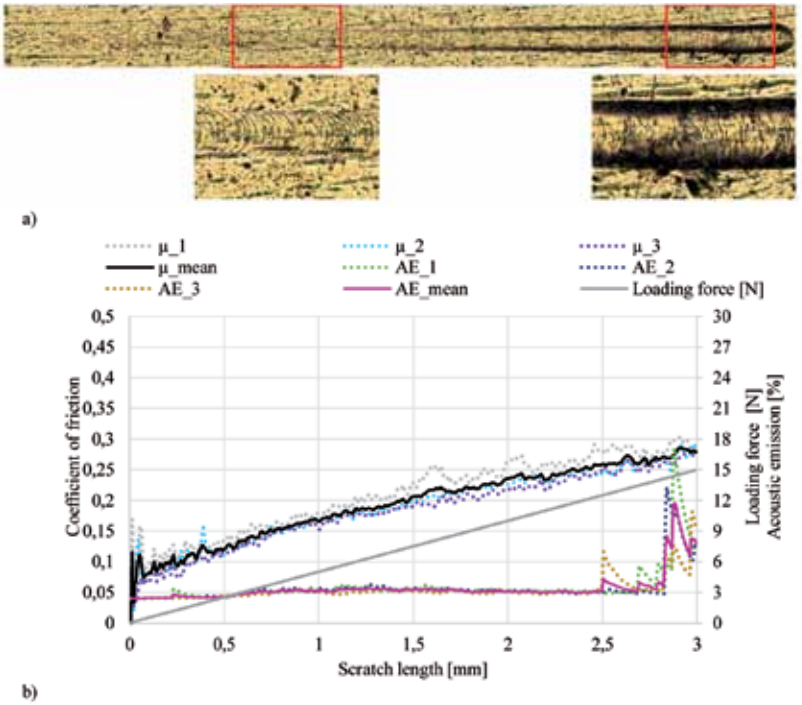

Fig. 6. Results of the scratch test (a), image of the scratch, (b) coefficient of friction and acoustic emission as a function of the scratch length

Rys. 6. Wyniki badań testu zarysowania a), obraz rysy, b) współczynnik tarcia oraz emisja akustyczna w funkcji długości rysy

The TiN:Ag coating is uniformly deposited overall surface of the Ti13Nb13Zr sample, as shown by the microscopic images of the cross sections. Based on the results, the TiN:Ag layer had a thickness of 5.54 µm, of which approximately 5.07 µm was the interlayer. Qualitative analysis has shown that the interlayer comprises titanium nitride (5c) and that silver is only present on the surface (5b).

The scratch test results of the TiN:Ag coating are shown in **Figure 6**. The tests were repeated three times. Based on microscopic observations, recorded changes in friction coefficient (µ) and acoustic emission (AE), the deposited layer was found to have high adhesion to the substrate.

The scratch test of the TiN:Ag coating showed that the coating did not delaminate as a result of the applied load. There were no characteristic jumps

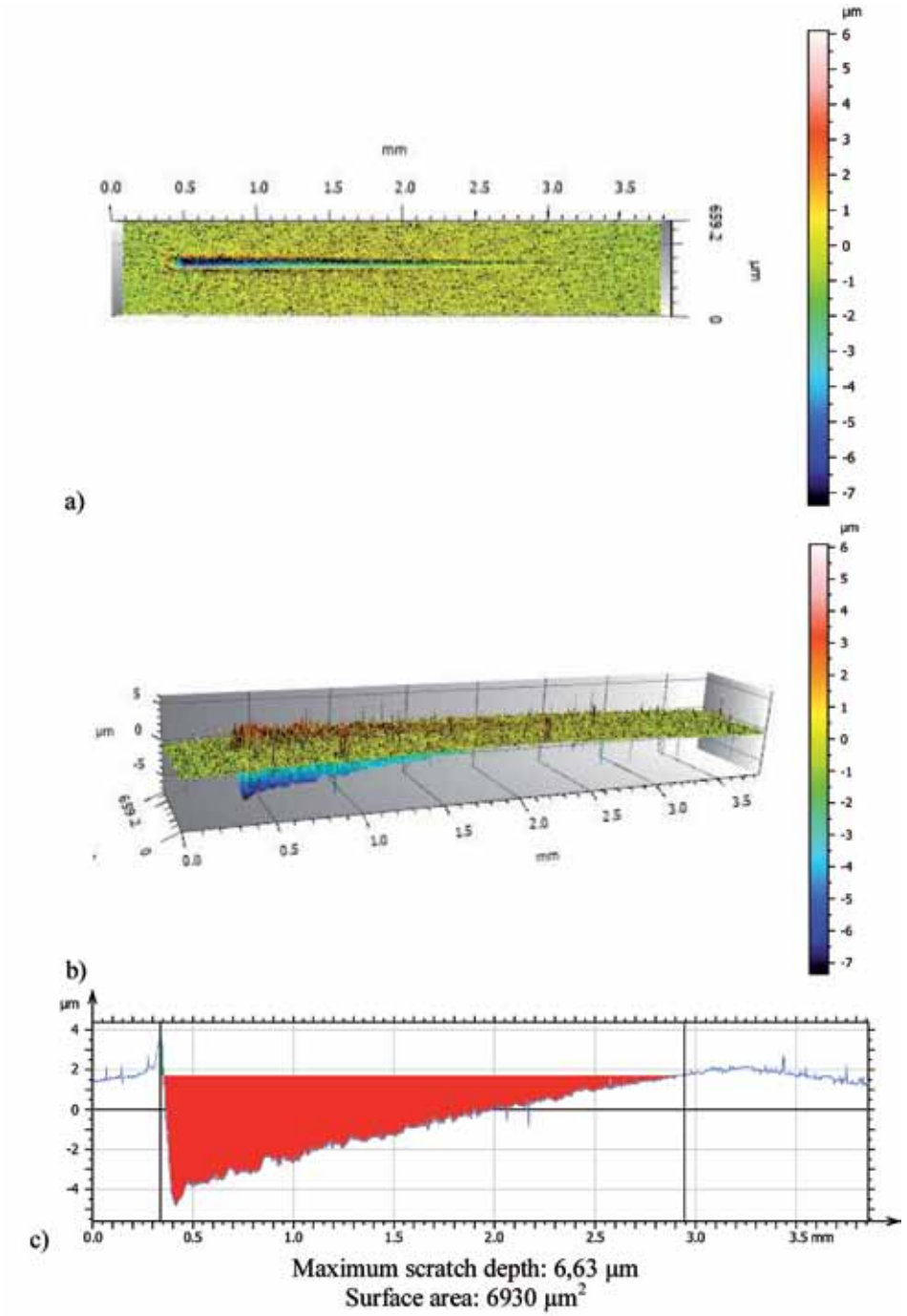

Fig. 7. 2D (a) and 3D (b) axonometric images of scratch test crack and longitudinal crack profile (c)

Rys. 7. Obraz aksonometryczny 2D (a) i 3D (b) rysy powstałej w wyniku testu zarysowania wraz z profilem rysy na przekroju wzdłużnym (c)

in the coefficient of friction curves to indicate chipping or peeling of the coating in any of the cases examined. In turn, the acoustic emission diagram showed that at a load of approximately 14.5 N, the first cracks in the coating began to appear. The measurement was repeated three times, and a characteristic peak was observed during each test. Based on the results, it has been concluded that the study should be extended with a higher load.

The cracks were examined microscopically after the adhesion tests. This was used to determine the average depth and area of the crack. The results are shown in **Figure 7**.

The scratches were examined under a microscope after the tests. These were used to determine the maximum depth of the crack and the area of the wear area. When the maximum load – 15 N – was applied, the indenter was at a depth of 6.63 μm, and, despite this, the deposited layer was not broken. This demonstrates the TiN:Ag coating's high elasticity.

Figure 8 shows the results of good runs of friction coefficients and average friction coefficients μ recorded during the cooperation of the friction pairs tested, counted based on three series of measurements.

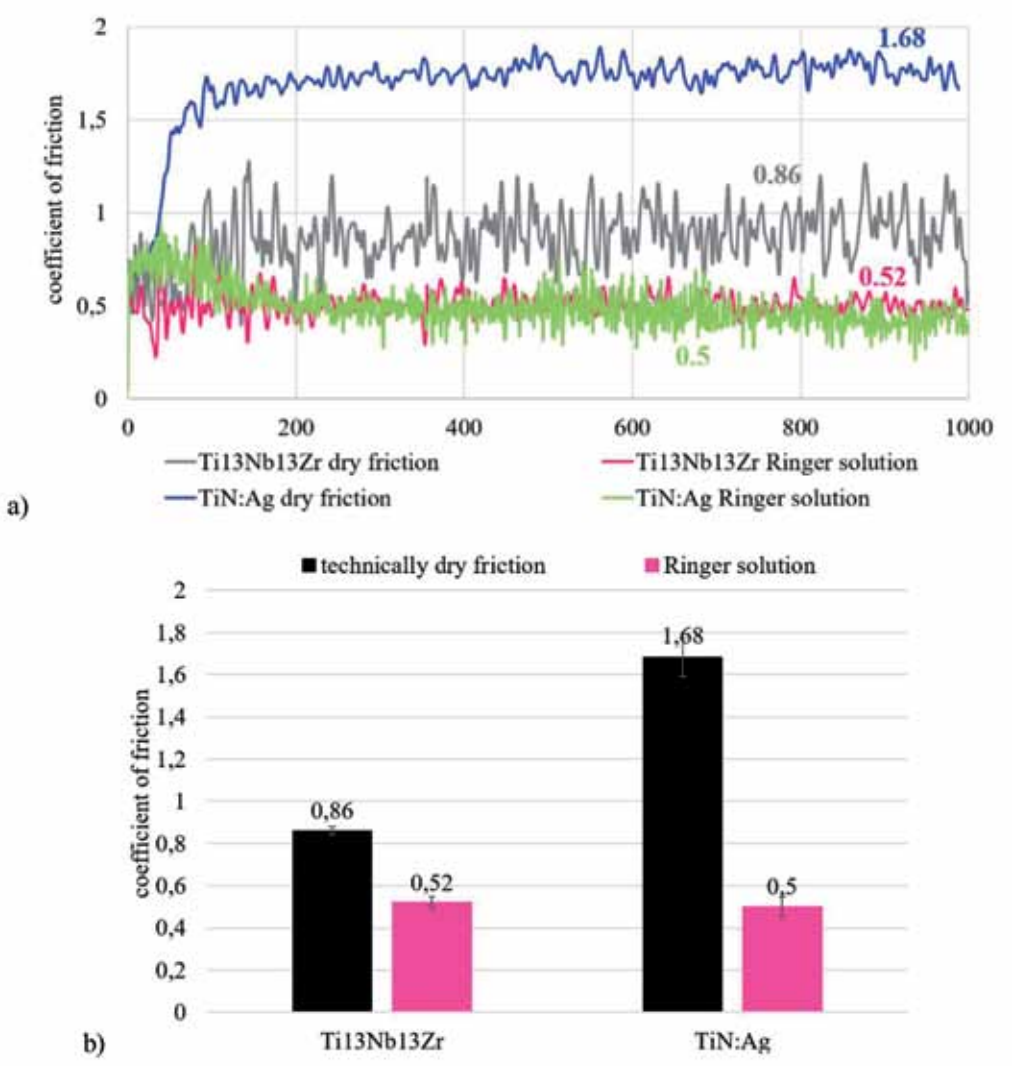

Fig. 8. Example of variation in friction coefficients (a), average friction coefficients (b)
Rys. 8. Przykładowy przebieg zmian współczynników tarcia (a), średnie współczynniki tarcia (b)

Tribological tests demonstrate the lubricant's positive effect on both friction pairs. The motional resistance recorded for the Ti13Nb13Zr titanium alloy was approximately 40% lower, and the TiN:Ag coating was 70% lower than the values obtained with technical dry friction. Furthermore, a significant effect of surface development/surface roughness on friction coefficient was observed.

The sample with the highest amplitude parameters (S_p, S_v, S_{sk}, S_{ku}) had the highest value coefficient of friction – 1.68.

The result of the interaction of frictional elements is tribological wear. Tribological wear is highly dependent on the stereometric properties of the surface. This applies both to tests carried out under dry friction conditions and to tests carried out with Ringer's fluid lubrication. Three series of measurements were used to determine the main wear $\bar{x}$ indicators: average wear area and standard deviation – σ. The results are shown in **Figure 9**.

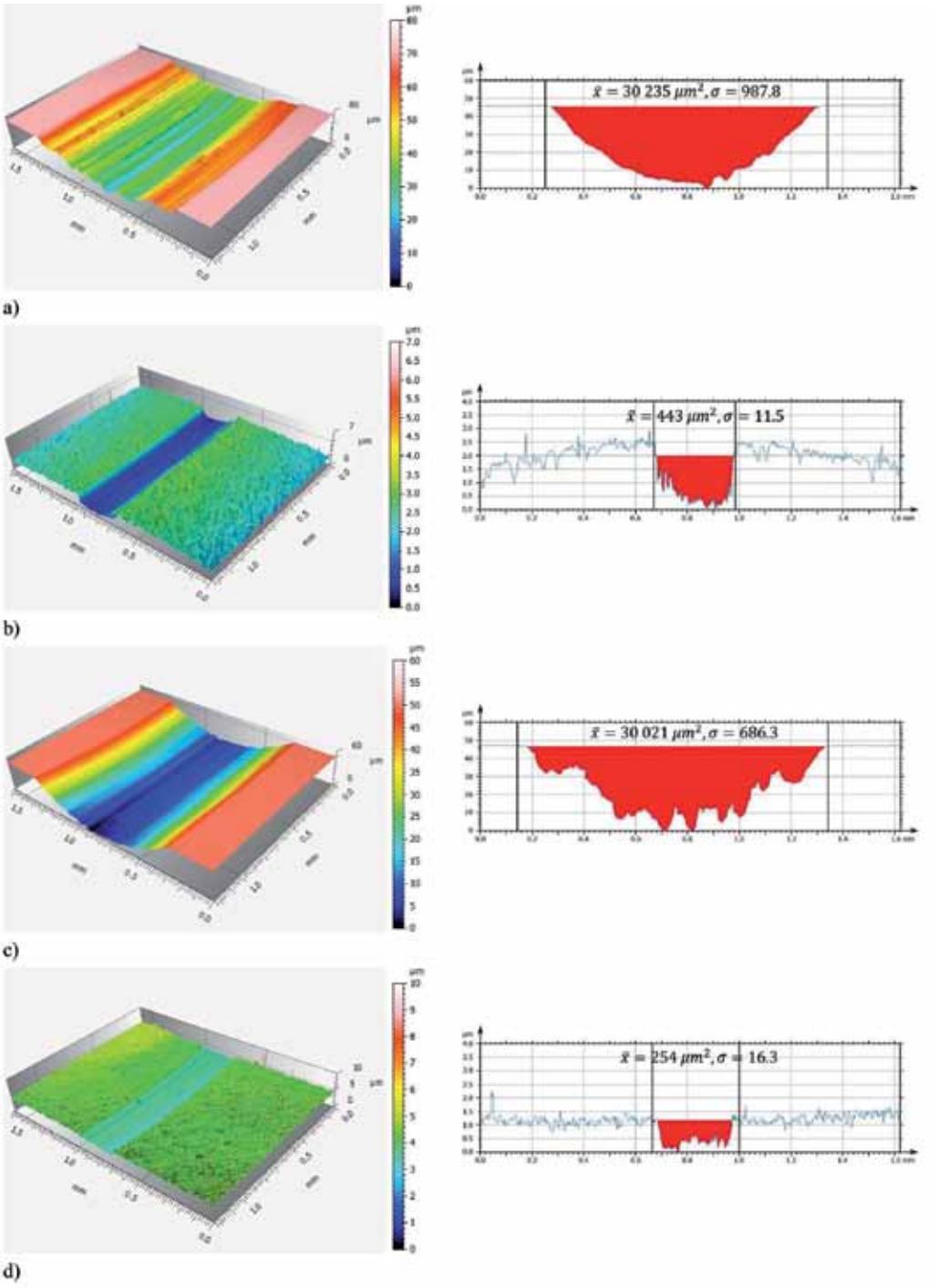

Fig. 9. The axonometric image of the trace of wear and the wear profile in a cross-section for dry friction: a) Ti13Nb13Zr, b) TiN: Ag, and friction in a Ringer's solution environment: c) Ti13Nb13Zr, d) TiN: Ag

Rys. 9. Obrazy aksonometryczne śladów wytarcia na przekroju poprzecznym podczas tarcia technicznie suchego: a) Ti13Nb13Zr, b) TiN:Ag, podczas tarcia ze smarowaniem roztworem Ringera c) Ti13Nb13Zr, d) TiN:Ag

Analysis of the microscopic results of the wear marks showed that there was a significant increase in the frictional wear resistance of the Ti13Nb13Zr alloy due to the deposition of the coating. It was also found that wear indicators, i.e., the maximum wear area on the cross-section, were reduced when Ringer's fluid was used as a lubricant. In the case of friction using Ringer's solution, the coating consumption was 254 μm^2 and was more than 40% lower compared to the values obtained in technically dry friction. Observing the wear marks also made it possible to identify the wear mechanism. In all cases studied, abrasive wear was predominant. The presence of characteristic grooves in the Ti13Nb13Zr specimens is due to hard Nb and Zr particles in the friction zone, further intensifying the wear process.

CONCLUSIONS

Advanced scanning microscopy was used to determine the thickness of the coating and the chemical composition of each layer. Based on the results of these tests, a coating of approximately 5.54 μm was deposited, the interlayer was TiN, and the silver was found mainly on the surface.

The deposited silver-doped titanium nitride layer showed high adhesion to the substrate, as shown by the adhesion test results. Microscopic observations of the crack showed that under 15 N loading, the indenter was at a depth of 6.6 μm, yet the coating did not break. This is evidence of the high strength of the coating.

The tribological tests and the observation of wear marks showed that the TiN: Ag coating had a higher wear resistance despite the high friction coefficients than the Ti13Nb13Zr alloy. For both the titanium alloy and the coating, the lubricant benefitted the frictional resistance – which was 40% and 70% lower, respectively, compared to technical dry friction.

REFERENCES

1. Chrobak A., Łagan S.: Analiza wybranych właściwości materiałów stosowanych na instrumentarium chirurgiczne, Aktualne problemy biomechaniki 2020, 19, pp. 5–11.
2. Eliaz N.: Corrosion of Metallic Biomaterials: A Review, Materials 2019, 12(3), p. 407.
3. Paszenda Z., Tyrlik-Held J.: Instrumentarium chirurgiczne. Wyd. Politechniki Śląskiej, Gliwice 2002, pp. 9–11.
4. Basiaga M., Paszenda Z.: Zastosowanie MES w analizie układu wiertło chirurgiczne – kość udowa, Aktualne problemy biomechaniki 2010, 4, pp. 17–22.
5. Marciniak J., Paszenda Z., Basiaga M., Smolik J.: Influence of carbon coatings on functional properties of surgical instruments, Engineering of Biomaterials 2007, 65–66, pp. 10–12.
6. Marciniak M.: Biomateriały, Wyd. Politechniki Śląskiej, Gliwice 2002.
7. Piotrowska K., Madej M., Ozimina D.: Assessment of the Functional Properties of 316L Steel Alloy Subjected to Ion Implantation Used in Biotribological Systems, Materials 2021, 14 (19).
8. Anderson C.G., Mikaberidze M., Gordeziani G., Gozalishvili E., Akhvlediani L., Dali R.: Corrosion Resistant Titanium Alloys for Medical Tools and Implants, Powder Metallurgy & Mining, 2013, 2 (2).
9. Więckowski W., Motyka M., Adamus J., Lacki P., Dyner M.: Numerical and Experimental Analysis of Titanium Sheet Forming for Medical Instrument Parts, Materials 2022, 15(5).
10. Piotrowska K., Madej M., Granek A.: Assessment of Mechanical and Tribological Properties of Diamond-Like Carbon Coatings on the Ti13Nb13Zr Alloy, Open Engineering 2020, 10, pp. 536–545.
11. Biel-Gołaska M.: Application of diamond layers and diamond-like coatings on medical tools and implants, Pr. Inst. Odlew. 2008, t. XLVIII, nr 2.
12. ASTM F1713-03 – standard specification for wrought Titanium-13Niobium-13Zirconium alloy for surgical implant applications.